communications earth & environment

ARTICLE

https://doi.org/10.1038/s43247-022-00535-1 OPEN

Increased carbon assimilation and efficient water usage may not compensate for carbon loss in European forests

Bruno Montibeller[1]✉, Michael Marshall[2], Ülo Mander[1] & Evelyn Uuemaa[1]

Phenological responses of vegetation to global warming impact ecosystem gross primary production and evapotranspiration. However, high resolution and large spatial scale observational evidence of such responses in undisturbed core forest areas is lacking. Here, we analyse MODIS satellite data to assess monthly trends in gross primary productivity and evapotranspiration across undisturbed core forest areas in Europe between 2000 and 2020. Both parameters increased during the early spring and late autumn in nearly half of the total undisturbed core forest area (3601.5 km2). Enhanced productivity drove increased water-use-efficiency (the ratio of gross primary productivity to evapotranspiration). However, productivity increases during spring and autumn were not sufficient to compensate for summertime decreases in 25% of core forest areas. Overall, 20% of total gross primary productivity across all European forest core areas was offset by forest areas that exhibited a net decrease in productivity.

[1] Department of Geography, University of Tartu, Tartu 51003, Estonia. [2] Faculty of Geo-Information Science and Earth Observation, University of Twente, Hengelosestraat 99, 7514 AE Enschede, the Netherlands. ✉email: bruno.montibeller@ut.ee

Forest ecosystems play an important role in global and regional carbon and hydrological cycles by acting as carbon sinks and as sources of water vapor via transpiration[1–4]. Photosynthesis drives the exchange of carbon and water between forest canopies and the ambient atmosphere. During photosynthesis, the trees assimilate atmospheric CO_2 as biomass, and release the soil water drawn from the roots back into the atmosphere as water vapor. Atmospheric CO2 assimilation sequesters up to 12% of anthropogenic carbon emissions, and transpiration is responsible for returning up to 40% of local precipitation to the atmosphere[5]. These processes mitigate anthropogenic CO2 emission and help to buffer rainfall patterns at various spatial scales[6–8] because of the returned water vapor back to the atmosphere.

The amount of carbon assimilated by an ecosystem during a given period is defined as gross primary production (GPP). The water lost during transpiration and evaporation from ecosystems is defined as evapotranspiration (ET). The dynamics of both are strongly driven by environmental conditions[9,10]. For example, global heating and extreme weather can directly alter forest GPP and ET[11–13]. GPP in temperate forests has increased in the spring and autumn because of the prolonged growing season triggered by global heating[14]. However, some studies have reported that the spring and autumn carbon gain is offset by carbon loss caused by higher summer respiration rates[15,16]. The warmer temperatures during spring and autumn can also increase the loss of soil moisture and plant transpiration, resulting in higher ET rates[17–19]. In summer, the higher ET rates can be linked to an increase in forest transpiration (which represent ~60% of land ET[5]) driven by warmer temperature and heat waves[20].

The trade-off between forest ecosystem GPP and ET is defined as water-use efficiency (WUE = GPP/ET)[21–23]. WUE per unit area increases as more carbon is gained and less water is lost. WUE has been widely used to assess forest–climate interactions[24–26], and especially forest responses to changing environmental conditions (e.g., precipitation declines, temperature rise, periodicity and intensity of droughts, CO2 fertilization)[16,27,28]. Several studies have used field-based data (e.g., eddy covariance flux tower, tree-ring isotopes) to evaluate local changes in forest WUE and GPP[29–31]. Other studies have used spaceborne Earth observation data to parameterize models that simulate GPP and WUE. The advantage of using Earth observation data is that it facilitates analysis of spatial and temporal trends in these variables over large forest areas at high spatial resolution. These analyses support the identification of areas within the forests that have shown increases or decreases in GPP, ET, and WUE[32–34]. These studies have provided insights on the environmental conditions drivers (e.g., increased leaf area index, rising atmospheric CO2 concentration) of the increased forest WUE and of the GPP compensation resulted from the trade-off between the GPP increase and the GPP decrease[32–34]. The GPP compensation occurs, for example, when the spring GPP increase offsets the summer GPP decrease). Other environmental conditions (e.g., soil water availability, vapor pressure deficit) and biotic variables (e.g., phenology, seasonality) have also been reported as factors that can promote or hinder GPP compensation[32,33].

To the best of our knowledge, there have been no high-resolution studies that focus on whether GPP increases or decreases in forested areas produce net carbon assimilation across seasons. Specifically, research has not identified which forest areas have experienced net GPP loss (e.g., the increased spring or autumn GPP does not compensate for decreased summer GPP) or net GPP gain (e.g., increased spring or autumn GPP offset or exceeded decreased summer GPP). Studies of GPP compensation have usually relied on seasonal GPP averages throughout a study region[32] or on the outputs of GPP models with coarse spatial resolution[16,33]. These approaches do not permit adequate analysis of intra-seasonal variation nor large-area spatial variation. In addition, there have been few studies that analyzed whether the potential seasonal increase of forest GPP is accompanied by an increase in WUE[21,35]. These studies indicated that GPP and WUE increase simultaneously due to a decrease in ET caused by elevated atmospheric CO2 effect on stomatal closure. Under elevated atmospheric CO2 concentrations, stomatal closure occurs to maintain a balance between CO2 uptake for photosynthesis and moisture loss. However, these studies[21,35] used mostly eddy-covariance measurements for WUE investigations at local forest sites without considering spatial variation over large forest areas and over long periods. Spatial analysis of seasonal forest GPP compensations and WUE dynamics at larger spatial scales is critically important for understanding the impact of climate change on forests and for application of management strategies that enhance net carbon assimilation[36–38].

In the present study, we investigated GPP, ET, and WUE trends in undisturbed temperate forest core areas (FCAs) in Europe and the Nordic countries (hereafter, "Europe" for simplicity). We focused on FCAs to avoid the edge effects that can alter the carbon cycle dynamic of the forest located within the edge[39], which would potentially introduce a spatial or temporal bias in our analysis. Specifically, we addressed the following questions: (i) What are the spatial and temporal trends of GPP, ET, and WUE in FCAs across Europe from 2000 to 2020? (ii) Is the temperature-driven increase in GPP during spring and autumn accompanied by an increase in WUE? (iii) Is the same FCA with GPP decrease and increase throughout the year showing an annual GPP gain or loss? (i.e., the increased spring and autumn GPP offset the decreased summer GPP). We hypothesized that (i) the spring and autumn GPP increase would not be accompanied by increased WUE in part of the FCAs because of a wide spread increase in ET over Europe[40]; and (ii) the GPP compensation across seasons would not necessarily occur in the same FCAs because of different forest responses to the varying environmental conditions across the large study area[32,33].

Results

European forest cover. The total undisturbed forest cover in Europe from 1986 to 2020 was 1.8×10^6 km^2 (Fig. 1a), distributed in more than 56×10^6 patches (average patch size of 3.3 ha). From this total, around 99.6% were located within a 500 m buffer from the forest edge and were removed from our analysis. Therefore, the remaining FCA was 6468.9 km^2 (0.4% of the total). Countries in eastern Europe (Poland, Croatia, Ukraine, Bosnia and Herzegovina, Belarus, and Romania) contained the largest area of FCA (Fig. 1). As we only analyzed the MODIS pixels with >50% of their area covered by FCAs, the final total forest area analyzed was 3601.5 km^2 (or 0.001% of the total undisturbed forest area in Europe).

Spatial and temporal trends of GPP, ET, and WUE. Our spatial and temporal analysis indicated that most of the FCAs showed no significant trend in GPP, ET and WUE (no significant trend in >85% of the FCAs for GPP, >76% for ET, and >62% for WUE; Supplementary Table 1) between 2000 and 2020. The few FCAs with significant increasing GPP trends were scattered throughout eastern, southern, and northern Europe (Fig. 2a), where most of the FCAs were located. These trends were most concentrated in early to mid-spring (March 12.1% and April 14.6% from the total FCA of 3601.5 km^2; Supplementary Table 1, Fig. 2b) and mid- to late autumn (October 5.2% and November 12.5%). On the other hand, the significant decreasing trends were concentrated in late spring (May 7.7%), early summer (June 3.8%), and early autumn (September 4.4%), and clustered in the south-eastern part of

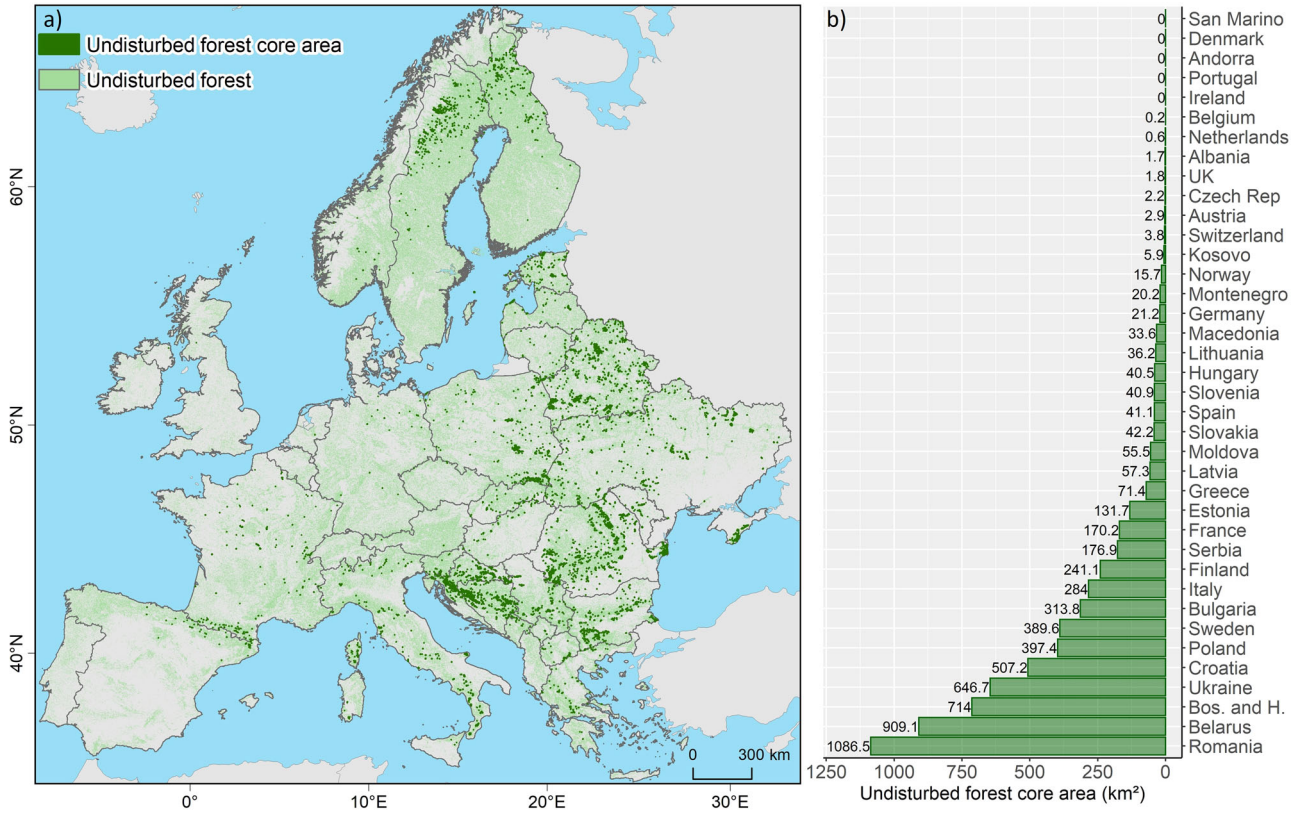

Fig. 1 Undisturbed forest cover and undisturbed forest core areas. a Spatial distributions of undisturbed forest cover and undisturbed forest core areas in 2020. **b** Undisturbed forest core area size by country in 2020. Forest core areas were >500 m from the edge of the undisturbed forest patches. Borders of the forest core areas have been exaggerated for visualization.

Europe. Comparing the median TS values for pixels with significant trends (Fig. 2c) revealed that the magnitudes of the decreasing TS values were greater than the magnitudes of the increasing TS values for most months (6 out of 9 months), especially in March (2.7 times) and November (4.2 times; Supplementary Table 2). However, we observed that the total annual GPP change for FCAs with increasing trends was 3.3 Mt C per year whereas the total for FCAs with decreasing trends was 2.0 Mt C per year (Fig. 2d). This result indicates that when considering the carbon trade-off between the FCAs with significant GPP trends, there is a net annual carbon gain of 1.3 Mt C per year. For the FCAs that showed no significant trend, the median monthly TS values indicated that May (-0.54 ± 1.05 gC m-2 year-1) and August (-0.06 ± 1 gC m-2 year-1) had negative TS trends and that the remaining months showed median TS values >0.05 gC m-2 year-1 (Supplementary Table 2, Supplementary Fig. 1).

In contrast with GPP, more FCAs showed significant increasing trends in ET than showed decreasing trends for all the months analyzed, except for May (Fig. 3). In May, the decreasing trends were clustered in southeastern Europe. June (16%), August (23.3%) and September (17.1%) showed the greatest proportion of FCAs with increasing trends (Supplementary Table 1). During June, August, and September, the FCAs with increasing trends for ET were mainly located in eastern Europe, whereas the remaining months showed no clear spatial pattern for the ET trends. We also observed that in contrast with GPP, FCAs with increasing ET trends had higher TS values than those with decreasing trends in most months (6 out of 9 months) (Fig. 3c and Supplementary Table 3). However, the difference between them was smaller (the ratio was close to 1) than the difference of the GPP TS values. As in the GPP analysis, the trade-off between the significant increasing and decreasing trends showed a net increase of ET (>2.1 million m3 of H2O per year) that was mainly driven by the positive values in June, August and September (Fig. 3d). Figure S2 shows the distribution of TS for ET throughout the study area.

The trend analyses for WUE showed that the FCAs with decreasing trends were spread throughout Europe, especially during the summer and early autumn, whereas FCAs with significant increasing trends were mainly clustered in eastern Europe during the spring and late autumn (Fig. 4a). The median TS values for FCAs with increasing trends in early spring and late autumn were at least 1.5 times greater than the TS values of FCAs with increasing trends in the remaining months (Supplementary Table 4). In terms of the area of FCAs (Fig. 4b), the area with increasing WUE was greater than the area with decreasing WUE in 5 months (May to September). TS in FCAs with a significant increase of WUE had a greater magnitude than in areas with a significant decrease in four of the nine months (Fig. 4c and Supplementary Table 4). Figure S3 shows the distribution of TS for WUE throughout the study area.

Interactions among GPP, ET, and WUE trends. By classifying the TS values of GPP, ET, and WUE into positive and negative trends, regardless of their statistical significance, we found that in early spring and late autumn, approximately half of the FCAs had increasing GPP, ET, and WUE (Fig. 5), reaffirming the previous results of significant trends. Therefore, the increase in WUE during these months did not result from decreasing ET rates but rather because the increase of GPP was greater than the increase of ET. In the summer, we observed the opposite pattern: more areas had increasing GPP (+) together with decreasing WUE. In most cases, GPP and WUE both decreased during the summer months due to increased ET.

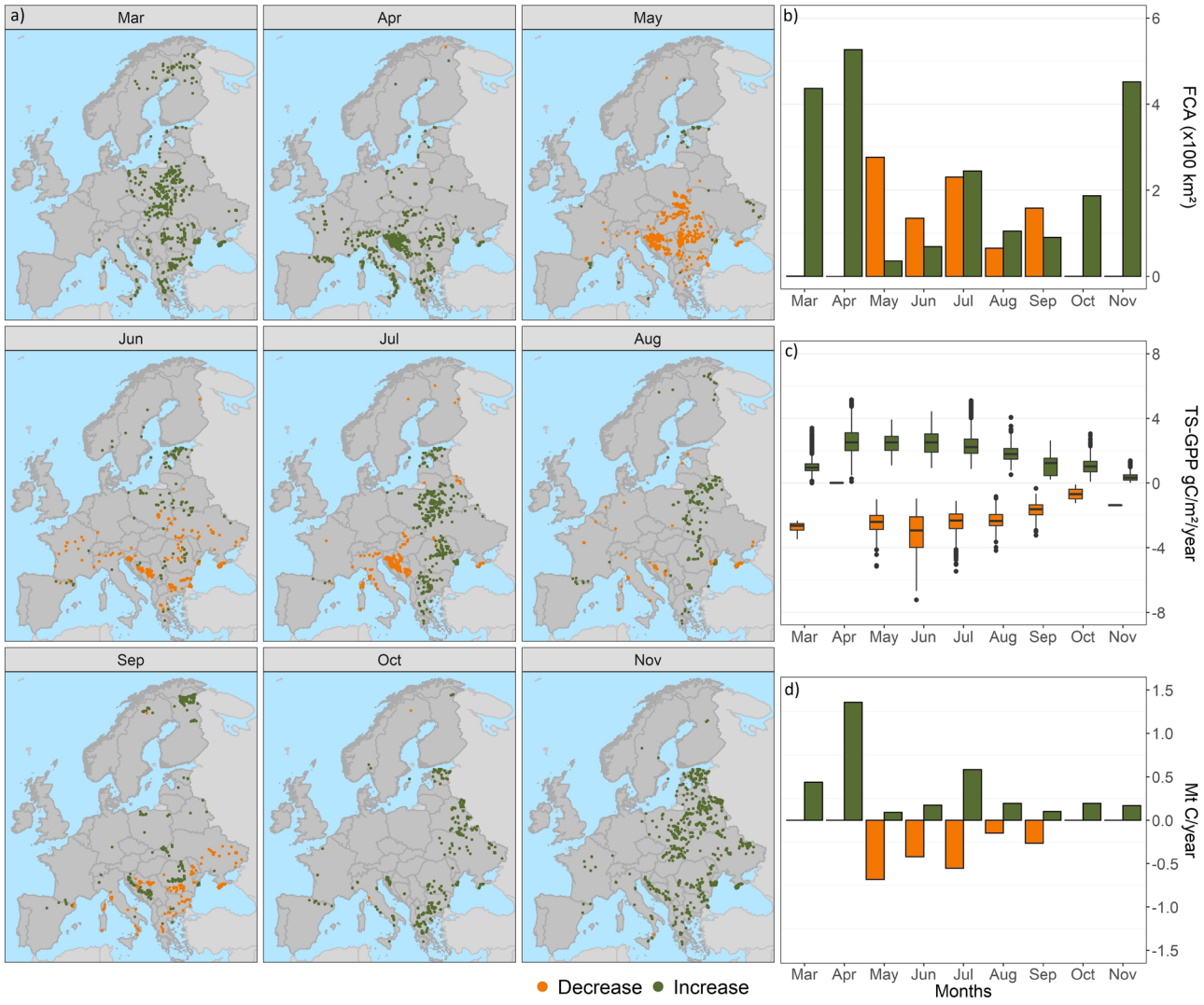

Fig. 2 Spatial and temporal dynamics of gross primary production over undisturbed forest core areas from 2000 to 2020. a Statistically significant (95% confidence interval) spatial and temporal trends for monthly gross primary production (GPP) of forest core areas (FCAs). **b** FCA areas that showed significant increases or decreases in GPP. **c** Theil–Sen's slope (TS) values for pixels with increasing and decreasing GPP trends at a monthly time step. **d** Monthly total carbon change for the increasing and decreasing GPP trends. Significant trends were identified using the Mann-Kendall test for each month.

GPP compensation. The monthly TS values for GPP revealed that >93% of the FCAs showed either a decrease or increase (significant or not) in at least one of the months analyzed (Supplementary Table 5). The month that showed the largest area of FCAs with increased GPP was November (98%). However, when calculating the total monthly GPP balance (total increase minus total decrease within the month), April showed the largest change (a net increase of 5 Mt per year; Fig. 6a). May, on the other hand, showed the largest area of FCAs with decreasing GPP (70%) and the largest negative GPP balance, at 2.3 Mt C per year (Fig. 6a). By summing the monthly GPP values at a pixel scale (i.e., multiplying the monthly TS values for GPP by the area of FCAs in a pixel), we found that 75.1% of the FCAs showed a net gain in GPP (increase minus decrease) of 9538.7 t C per year (Fig. 6b). For the remaining 24.9% of the FCAs that showed decreased GPP, the total net loss was 1960.8 t C per year (Fig. 6b). Thus, the net carbon balance for GPP in the FCAs was 7577.9 t C per year. The FCAs with net loss in GPP were clustered in northern and southern Europe (Fig. 6c), whereas FCAs with net gain in GPP were scattered throughout Europe (Fig. 6d).

Discussion

Many studies across ecosystems have shown that GPP increases during spring and autumn[32,33,41]. However, there have not been many studies that focused on whether this GPP increase was accompanied by an increase in WUE, especially for undisturbed forest ecosystems. Moreover, there have been even fewer studies of whether the GPP increase can compensate for the GPP decrease in a forest area that shows both trends during different months. Using spatial data for Europe obtained over a 20-year period, we quantified monthly trends (increasing and decreasing) and rates of change for GPP, ET, and WUE across undisturbed FCAs. The novelty of our findings is that most of these FCAs showed a simultaneous increase in GPP and WUE, despite the concurrent increase in ET. Therefore, the increase in WUE was because of a greater GPP increase than the increase in ET. We also found that 25% of the FCAs that showed both increases and decreases in GPP during the year showed no GPP compensation (i.e., the GPP increase permitted by a prolonged growing season did not offset the GPP decrease).

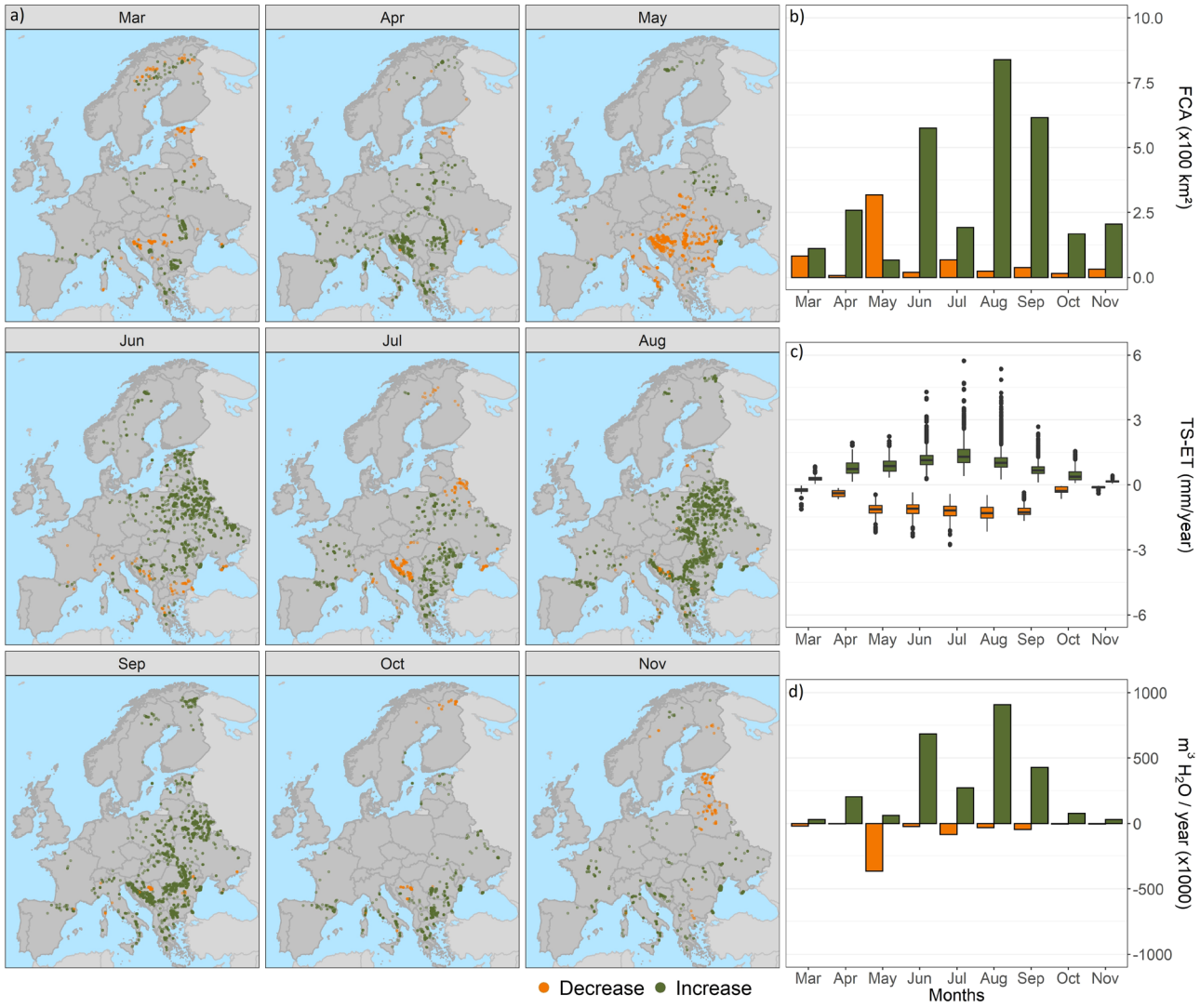

Fig. 3 Spatial and temporal dynamics of evapotranspiration over undisturbed forest core areas from 2000 to 2020. a Distributions of forest core areas (FCAs) with statistically significant ($p < 0.05$) increasing or decreasing trends for monthly evapotranspiration (ET) from 2000 to 2020. **b** Total FCA area that showed a significant increase or decrease in ET. **c** Theil–Sen's slope (TS) values for the increasing and decreasing ET trends at a monthly time scale. **d** Monthly total ET trend (increase and decrease). Significant trends were identified using the Mann–Kendal test for each month.

The WUE increase was not linked to an ET decrease. Our results for GPP increases and decreases agree with the literature in which climate change, a longer growing season, and the CO_2 fertilization effect potentially altered forest productivity dynamics[14,34,42]. The heating-induced change in the phenology of temperate forests and increases in the CO_2 concentration is likely driven by the spring productivity increase, whereas the summer productivity decrease is likely driven by changes in climate extremes (e.g., drought or heat wave)[14,16]. Eddy-covariance data indicated that the increase of carbon uptake (GPP) during spring and autumn was greater than the carbon released by forest respiration despite the heating trends identified in both seasons[14]. This finding agrees with our results, which showed a WUE increase during these seasons. We observed that approximately half of the FCAs showed increases in both GPP and WUE, despite the increased ET during the early spring and late autumn (Fig. 5). This indicates that the rate of increase of GPP was higher than the rate of increase of ET, which includes not only the water from evaporation in the forest ecosystem but also losses from the vegetation's respiration and transpiration. Therefore, our WUE analysis provided additional critical information, namely that this simultaneous increase did not result from decreased ET[21,43], but rather from the greater increase of GPP. Our WUE analysis also showed that the concomitant GPP and WUE increases in early spring and late autumn were widespread and affected >70% of the FCAs.

A WUE increase during spring and autumn, which has been identified by other studies in the last decade[21,35,44], has also been linked to an increase in the concentration of atmospheric CO_2. Under elevated CO_2 concentrations, forests and other C3 vegetation photosynthesize more and can decrease their stomatal apertures to prevent the loss of water vapor during transpiration, which leads to an increase in WUE[45]. Nevertheless, it is important to note that the influence of the atmospheric CO_2 concentration on the magnitude and direction of changes in WUE is still debated[21,30,34,44–49]. Moreover, during summer months, most of the FCAs showed significant decreases in WUE (Fig. 4b) because of higher ET. During warmer summers and heat waves periods, the vegetation reduces the carbon uptake activity (and therefore also GPP) to prevent water loss driven by high vapor pressure deficit[50]. However, other studies have found that, under these weather conditions, forest areas can increase

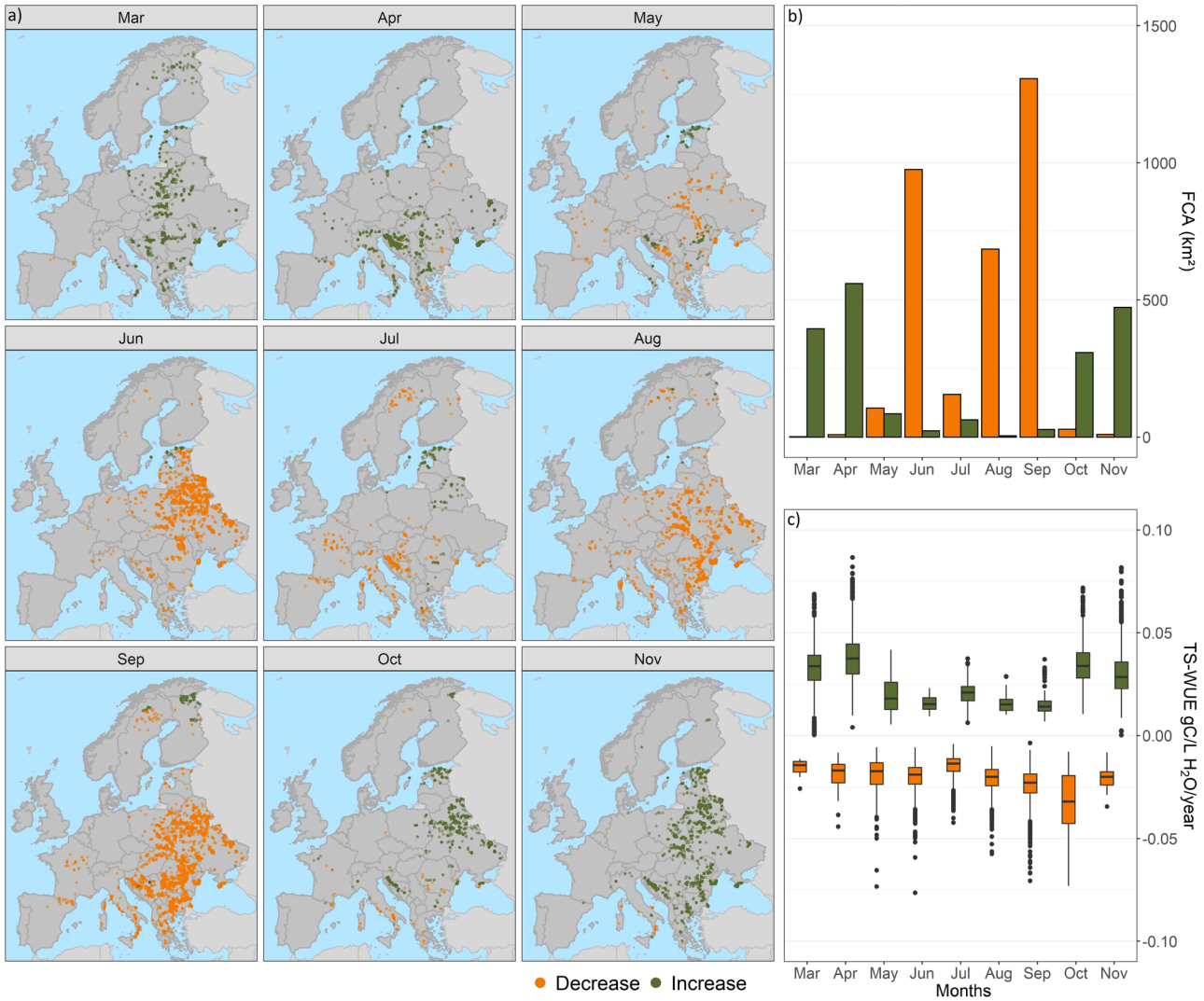

Fig. 4 Spatial and temporal dynamics of water-use-efficiency over undisturbed forest core areas from 2000 to 2020. a Distributions of forest core areas (FCAs) with statistically significant ($p < 0.05$) increasing or decreasing trends for monthly-scale water-use efficiency (WUE) from 2000 to 2020. **b** Total area of FCAs with significant increases or decreases in WUE. **c** Theil–Sen's slope (TS) values for increasing and decreasing WUE trends at monthly time scale. Significant trends were identified using the Mann–Kendal test for each month.

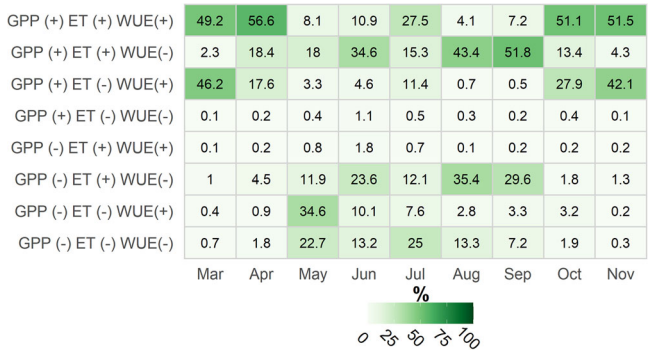

Fig. 5 Proportion of forest core areas based on the interaction among gross primary production, evapotranspiration, and water-use-efficiency. Proportions (%) of the total forest core areas (FCA) that showed an increase (+) or decrease (-) in gross primary production (GPP), evapotranspiration (ET), and water-use efficiency (WUE).

transpiration[51] (~60% of land ET[5]) to cool the canopy[20]. These findings corroborate the observed higher ET rates and decrease WUE during summer in our analysis.

Forest type is another important factor that affects the changing rates and spatial distribution of the GPP and WUE trends. For instance, deciduous broadleaf forests show a greater increase in WUE than evergreen needleleaf forests in the northern hemisphere[35]. The WUE increase for deciduous broadleaf forests results mainly from decreased stomatal conductance, accompanied by decreased respiration, which affects ET rates. In contrast, the GPP increase was the main driver for the increased WUE of evergreen needleleaf forests[35]. These findings are aligned with our results. The deciduous broadleaf forests, which are dominant in southern Europe (Supplementary Fig. 4)[52], also showed higher increase in WUE (Supplementary Fig. 3) than the evergreen needleleaf forests, which are dominant in central and northern Europe (Supplementary Fig. 4)[52]. These differences in the GPP rates between forest types, combined with soil properties (e.g., water availability, fertility), relief (e.g., slope) and forest age, can also explain why adjacent FCAs may show divergent GPP trends (increase and decrease).

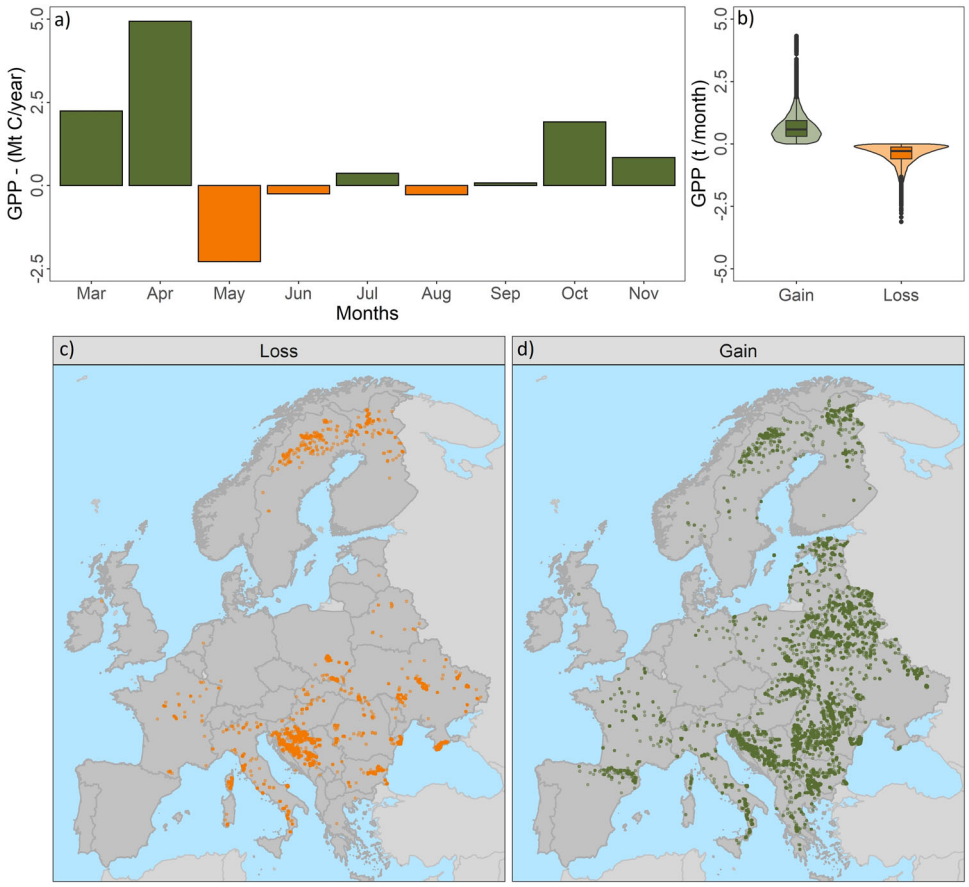

Fig. 6 Temporal and spatial gross primary production balance of forest core areas. a Gross primary production (GPP) compensation (total increase minus total decrease) for forest core areas (FCAs) at a monthly time step. **b** Boxplots of the annual net GPP gain and loss for all FCAs across Europe, where the black horizontal lines are the medias, and the shaded area is the frequency of the values. **c** Spatial distribution of FCAs with annual net GPP loss. **d** Spatial distribution of FCAs with annual net GPP gain.

Although the observed increases in GPP and WUE currently have a beneficial effect on the carbon and water balance of forests, some studies suggest that these trends might change in the future[9,41]. For example, Reyer et al.[53] predicted that the annual forest productivity will increase in northern Europe, increase in some parts of central Europe and decrease in others, and decrease in southern Europe. These predictions are concerning because we observed that the rates of GPP increase in northern Europe were lower than the rates of GPP decrease in central and southern Europe (Supplementary Fig. 1). Hence, the potential for GPP compensation between the two regions is unlikely. Moreover, the forests in south-eastern Europe are frequently affected by drought-related mortality[54] that would further reduce the potential for GPP compensation by northern European forests.

Annual compensation of GPP. We found that approximately 25% of the FCAs showed an annual GPP loss. These FCAs showed both increases and decreases in GPP during different months, but overall presented no GPP compensation (i.e., the GPP gains did not offset the GPP losses), as we hypothesized. For most of these FCA, the lack of GPP compensation resulted from the GPP decrease during summer. This decrease of GPP is probably linked to the increase in temperature, to the decrease in precipitation and to the increase occurrence of dry and hot periods, as reported by other studies[40,55,56]. Under these weather conditions, water vapor pressure deficit can increase, and water soil availability can decrease[50,57]. The combination of these factors induce a reduction in stomatal conductance by the vegetation which results in a decline of the photosynthesis activity and, therefore, decreases the GPP rates[46,58]. Previous studies have reported different inter-seasonal compensation in GPP across different ecosystems[16,32,59]. However, these reports did not focus on forest areas, covered short periods (e.g., 5 years), and did not have high spatial resolution. We identified the location of the FCAs that showed no GPP compensation. The locations of these areas suggest that they are spread through different forest types (coniferous and broadleaf forests) based on the CORINE land cover map[52] and are spread across Europe (Fig. 6c, d). Therefore, our results provide insights for the application of forest management techniques (e.g., shelterwood cutting, thinning) over FCAs with net GPP loss that enhance carbon assimilation[60,61] and promote the achievement of GPP compensation.

By summing the total GPP increases and decreases across all FCAs in Europe, we found that the FCAs with a GPP loss were responsible for offsetting 20% of the total GPP increase across the continent. This percentage could increase in the future, as some studies have indicated that in the next 20 to 30 years, ecosystems–including forests– may reach a productivity tipping point[62,63]. At that point, the forest areas may show a productivity reduction that would further exacerbate the reduction of GPP compensation.

Implications for carbon and water cycles. In contribution to previous studies focused on the impact of deforestation and forest degradation on the carbon and water cycles, our study highlighted two key impacts that the FCAs may have on these cycles.

First, more carbon is being assimilated (GPP) per liter of water (i.e., improved WUE) during the early spring and late autumn. However, this efficiency has not resulted from decreased water loss (ET). On the contrary, most of the FCAs showed an increase in ET (Fig. 5) that can affect regional water cycles[34]. For instance, to maintain the spring GPP increase, the vegetation removes water from the soil, which is not replaced because of reduced precipitation during the spring[64]. Therefore, the increase in ET during this season can decrease soil moisture in the summer[18], and if this is combined with more frequent summer droughts[65], it will further hinder any potential GPP increase. Second, part of the FCAs (25%) showed a net loss in GPP (i.e., the GPP loss outweighed the GPP gains), suggesting that certain forest areas do not act as carbon sink. This is particularly concerning because climate change is predicted to decrease forest productivity[53], further decreasing the potential GPP compensation. In addition, these dynamics can also affect the potential of certain forest areas to be considered for nature-based solutions for climate change mitigation.

Our study has some limitations. First, because GPP includes carbon loss from foliar respiration from above ground vegetation[66], as well as autotrophic and heterotrophic respiration from soil[67], we acknowledge that our results do not directly report the decrease or increase of carbon accumulation as biomass. That would be represented by net primary production (NPP), which is also provided as a MODIS product but on an annual basis. Nevertheless, previous studies indicated a relatively constant ratio of NPP to GPP (0.46 ± 0.12)[68,69] across different biomes, tree species, and forest stand ages. Thus, our GPP results can be used as a proxy for understanding the role of forest areas as carbon sinks or sources at monthly time scale. Second, although we validated the GPP and ET MODIS products using ground-based eddy covariance data (Supplementary Fig. 5), the coarse resolution of the satellite products can limit accurate estimation of these variables and miss variations in the forest composition at a subpixel scale that would affect the rate of carbon assimilation. Therefore, future work should focus on improving the forest GPP and ET analysis by integrating the high-resolution forest disturbance maps used in the present study with recently developed high-resolution forest type maps[70]. Data-driven models (e.g., machine learning models) or process-based models could be applied to improve the estimation of GPP and ET, using environmental covariates (e.g., atmospheric relative humidity) retrieved specifically for the forest areas. The GPP and ET estimations could be also done both with higher spatial resolution and stratified by forest types. Moreover, the data-drive models could also use climate variables as covariates (e.g., temperature, precipitation, vapor pressure deficit) and analysis could then be performed to provide insights about the GPP, ET and WUE response to climate extremes. Third, we did not scrutinize the uncertainties in GPP, ET and WUE trends and rates beyond our flux tower evaluation of MODIS GPP and ET. We could have approached uncertainty with ensemble modeling. Ensemble modeling benefits from a number of products with considerably different architectures[71]. In our case, there are only two other products[72,73] with a suitable spatial resolution to address forest core areas. One of the products is very similar to the MODIS GPP/ET products[72]. Therefore, we recommend uncertainty analysis as future work in case more appropriate and comparable GPP and ET products become available. We attempted to validate WUE with the eddy covariance data. However, several spurious values were observed that prevented a realistic assessment. Unrealistic values have been reported in other studies[28,74] and were attributed to the differences of how GPP and ET are retrieved from flux towers measurements. Fourth, the use of higher resolution remote sensing images could also improve analyses of GPP and ET dynamics at forest edges. Analysis of these variables that accounts for the age of the forest edges is essential, not only because most of the undisturbed European forest areas are located within 500 m from the edge of the forest, but also to account for carbon losses that are perhaps missing from national carbon emission estimations[39].

Despite these limitations, our results suggest that carbon assimilation and the efficiency of water use during spring and autumn have increased. However, these increases may not compensate for increased summer carbon losses (or decreased summer gains) under climate change (hotter and dryer summers). Our spatially explicit analysis of GPP, ET, and WUE will support the development and improvement of forest management strategies that focus on climate adaptation to increase carbon assimilation. Specially, in southern and eastern Europe, where FCAs show greater rates of GPP increase or decrease than in other FCAs during the same months (Supplementary Fig. 1). Therefore, these FCAs appear to be critically important areas for efforts to achieve GPP compensation. In addition, our results provide insights into the role that undisturbed European forests will play in achieving the greenhouse gas emission reductions targets established under the Paris Agreement[75].

Materials and methods

Forest cover. We quantified forest cover dynamics using forest cover and forest disturbance maps with 30-m spatial resolution[76]. The authors[76] used Landsat satellite image time series and the LandTrendr[77] algorithm to map annual forest disturbance in Europe between 1986 and 2020. Using 5000 reference pixels that were manually interpreted by a team of image interpretation experts, the authors reported an overall map accuracy of 92%.

To retrieve the undisturbed FCAs in Europe, we overlaid the forest cover map and the annual disturbance maps[76] and removed all forest areas that showed any type of disturbance from 1986 to 2020. Therefore, the undisturbed FCAs that we investigated were at least 34 years old. In addition, we removed the forest edges from our analysis by applying an inner buffer of 500 m (the MODIS spatial resolution; see the next section for details) to avoid edge effects[39,78]. The edge effects can change abiotic conditions[78] and modify the forest dynamics (e.g., carbon assimilation rates)[39] in trees growing at forest edges. Thus, forest edges were considered as disturbed forest areas and could affect or bias our analysis. Therefore, these areas were removed.

The forest types within the FCAs ranged from pure stands of boreal conifers in the north to stands dominated by deciduous broadleaf trees in the south. Since our goal was to quantify overall changes of carbon assimilation by European forests, we did not attempt to stratify our analysis by forest type. This would be difficult given the (i) lack of high-resolution data that provides forest type information and (ii) the resolution (500 m) of the satellite data used for GPP and ET models would make it difficult to assign the correct proportions of these variables to each forest type.

MODIS *ET* and *GPP* data products. We estimated *GPP* and *ET* from 2000 to 2020 at a 500-m spatial resolution using the 8-day gap-filled MODIS composites (version 6) developed by the National Aeronautics and Space Administration: MOD16A2GF and MOD17A2HGF (Extracting and Exploring Analysis Ready Samples; https://lpdaacsvc.cr.usgs.gov/appeears/). The *ET* MODIS model consists of a series of ecophysiological constraints on atmospheric moisture demand or potential evapotranspiration as defined by the Penman-Monteith equation[79,80]. Similarly, the *GPP* MODIS model uses ecophysiological parameters to down-regulate carbon assimilation driven by incoming solar radiation[81,82]. The ET composites represent the sum of *ET* (kg H_2O m-2) while the GPP composites represent the sum of *GPP* (kg C m-2) over the 8-days period. Both MODIS products have been improved compared to the previous collection because poor-quality pixels (e.g., pixels contaminated by cloud cover or aerosols) have been eliminated and the gaps were filled through linear interpolation[83,84].

We used the composites that spanned the boreal spring, summer, and autumn months (March to November). The composites from December, January, and February were excluded for the following reasons: (i) At high latitudes, which included a large part of our study area, the *ET* and *GPP* rates in these months are negligible. (ii) Data were missing for *ET* and *GPP* 8-days composites in January and February of 2000 and 2016.

We removed all MODIS pixels that did not fall within the area identified as an FCA and used only pixels that had continuous times series for *ET* and *GPP* values throughout the study period (2000 to 2020). We used the monthly *ET* and *GPP* values in the trend analysis to investigate intra-season variability.

We evaluated the quality of the MODIS *GPP* and *ET* products for our analysis using the *GPP* and *ET* data acquired by 16 flux towers established in forested areas

throughout Europe (Supplementary Fig. 4). The data were compiled from the FLUXNET dataset[85]. The results indicated good agreement between the MODIS *GPP* and the FLUXNET GPP ($R^2 = 0.74$, $p < 0.05$; RMSE: 72.31 gC m-2 month-1; see Supplementary Fig. 5A) and between the MODIS *ET* and the FLUXNET ET ($R^2 = 0.67$, $p < 0.05$; RMSE = 24.3 mm month-1; see Supplementary Fig. 5B). Additionally, we also compared the MODIS GPP and ET with the estimations generated based on the PML-V2 model[73] to assess the robustness of the MODIS products. The comparison was made using the variables values acquired at the tower locations. The results also indicated good agreement for GPP ($R^2 = 0.84$, $p < 0.05$; RMSE: 44.79 gC m-2 month; see Supplementary Fig. 6A) and ET ($R^2 = 0.8$, $p < 0.05$; RMSE = 24.15 mm month-1; see Supplementary Fig. 6B).

Spatial analysis. We calculated the core forest fraction within the MODIS pixels to analyse the monthly trends in *GPP*, *ET*, and *WUE*. We selected all the MODIS pixels with >50% (>12.5 ha) of their area covered by FCAs for our analysis. We used this area threshold, which has been used in other studies[86,87], to increase the signal to noise ratio. In total, we analysed 18539 MODIS pixels totaling 360, 150 ha of FCA.

Trend analysis. We used the Theil–Sen slope (*TS*) to capture the rate of change in *GPP*, *ET*, and *WUE* at a monthly time scale[88,89]. *TS* is the median value of the slopes from all pairwise combinations within a time series. Based on the *TS* values, we identified the FCAs that showed any of the following combinations in GPP, ET and WUE rates (+ for increasing rates, – for decreasing rates). These combinations were set regardless the statistical significance of the rates of change:

(i) *GPP* (+) *ET* (+) *WUE* (+)
(ii) *GPP* (+) *ET* (–) *WUE* (+)
(iii) *GPP* (+) *ET* (–) *WUE* (–)
(iv) *GPP* (+) *ET* (+) *WUE* (–)
(v) *GPP* (–) *ET* (–) *WUE* (–)
(vi) *GPP* (–) *ET* (+) *WUE* (+)
(vii) *GPP* (–) *ET* (+) *WUE* (–)
(viii) *GPP* (–) *ET* (–) *WUE* (+).

As the monthly *TS* values of *GPP* indicate the rate of change in gC m-2 month-1, we multiplied the monthly *TS* values by the area of FCAs within each MODIS pixel to retrieve the total carbon increase or decrease in the respective pixel for the respective month. Then, we summed the total monthly carbon values for every pixel. We used these sums to identify the FCAs with an annual *GPP* loss or gain. The FCAs with a *GPP* gain represent areas where the *GPP* increase in spring and autumn compensated for (offset) the summer *GPP* decrease. However, if the FCA showed *GPP* loss, the *GPP* increase did not offset the *GPP* decrease.

We used the non-parametric Mann–Kendall test[90,91] to identify the spatial location of the FCAs with significant monthly trends in the *GPP*, *ET*, and *WUE* time series. This approach has been widely used in trend analysis of various Earth observation–based environmental indicators[46,49,92]. We masked significant trends using the 95% confidence band ($p < 0.05$).

Data availability

All datasets used in this current study have been acquired from the following open sources: Forest cover and disturbance maps from https://zenodo.org/record/4570157; MODIS GPP and ET version 6 products from https://lpdaacsvc.cr.usgs.gov/appeears/; and FLUXNET tower measurements from https://fluxnet.org/data/download-data/.

Code availability

The codes used to perform the analyses and create most of the figures are available via GitHub (https://github.com/brunomontibeller/GPP_WUE_forest_areas).

Received: 26 January 2022; Accepted: 16 August 2022;
Published online: 29 August 2022

References

1. Ellison, D. et al. Trees, forests and water: cool insights for a hot world. *Glob. Environ. Chang.* **43**, 51–61 (2017).
2. Pugh, T. A. M. et al. Role of forest regrowth in global carbon sink dynamics. *Proc. Natl. Acad. Sci. USA.* **116**, 4382–4387 (2019).
3. Harris, N. L. et al. Global maps of twenty-first century forest carbon fluxes. *Nat. Clim. Chang.* https://doi.org/10.1038/s41558-020-00976-6 (2021).
4. Aragão, L. E. O. C. The rainforest's water pump. *Nature* **489**, 217–218 (2012).
5. Schlesinger, W. H. & Jasechko, S. Transpiration in the global water cycle. *Agric. For. Meteorol.* **189–190**, 115–117 (2014).
6. Makarieva, A. M., Gorshkov, V. G. & Li, B. L. Revisiting forest impact on atmospheric water vapor transport and precipitation. *Theor. Appl. Climatol.* **111**, 79–96 (2013).
7. Staal, A. et al. Forest-rainfall cascades buffer against drought across the Amazon. *Nat. Clim. Chang.* **8**, 539–543 (2018).
8. Grassi, G. et al. The key role of forests in meeting climate targets requires science for credible mitigation. *Nat. Clim. Chang.* **7**, 220–226 (2017).
9. Zohner, C. M., Mo, L., Pugh, T. A. M., Bastin, J. F. & Crowther, T. W. Interactive climate factors restrict future increases in spring productivity of temperate and boreal trees. *Glob. Chang. Biol.* **26**, 4042–4055 (2020).
10. Hatfield, J. L. & Dold, C. Water-use efficiency: Advances and challenges in a changing climate. *Front. Plant Sci.* **10**, 1–14 (2019).
11. Grossiord, C. et al. Warming combined with more extreme precipitation regimes modifies the water sources used by trees. *New Phytol* **213**, 584–596 (2017).
12. Ruiz-Pérez, G. & Vico, G. Effects of Temperature and Water Availability on Northern European Boreal Forests. *Front. For. Glob. Chang.* **3**, 1–18 (2020).
13. Luo, X. et al. The impact of the 2015/2016 El Niño on global photosynthesis using satellite remote sensing. *Philos. Trans. R. Soc. B Biol. Sci.* **373**, 1–12 (2018).
14. Keenan, T. F. et al. Net carbon uptake has increased through warming-induced changes in temperate forest phenology. *Nat. Clim. Chang.* **4**, 598–604 (2014).
15. Oishi, A. C. et al. Warmer temperatures reduce net carbon uptake, but do not affect water use, in a mature southern Appalachian forest. *Agric. For. Meteorol.* **252**, 269–282 (2018).
16. Sippel, S. et al. Contrasting and interacting changes in simulated spring and summer carbon cycle extremes in European ecosystems. *Environ. Res. Lett.* **12**, 1–14 (2017).
17. Gaertner, B. A. et al. Climate, forest growing season, and evapotranspiration changes in the central Appalachian Mountains, USA. *Sci. Total Environ.* **650**, 1371–1381 (2019).
18. Lian, X. et al. Summer soil drying exacerbated by earlier spring greening of northern vegetation. *Sci. Adv.* **6**, eaax0255 (2020).
19. Harrison, J. L. et al. Growing-season warming and winter soil freeze/thaw cycles increase transpiration in a northern hardwood forest. *Ecology* **101**, 1–16 (2020).
20. De Kauwe, M. G. et al. Examining the evidence for decoupling between photosynthesis and transpiration during heat extremes. *Biogeosciences* **16**, 903–916 (2019).
21. Jiang, Y. et al. Trends and controls on water-use efficiency of an old-growth coniferous forest in the Pacific Northwest. *Environ. Res. Lett.* **14**, (2019).
22. Yu, Z. et al. Natural forests exhibit higher carbon sequestration and lower water consumption than planted forests in China. *Glob. Chang. Biol.* **25**, 68–77 (2019).
23. Dong, G. et al. Non-climatic component provoked substantial spatiotemporal changes of carbon and water use efficiency on the Mongolian Plateau. *Environ. Res. Lett.* **15**, 095009 (2020).
24. Belmecheri, S. et al. Precipitation alters the CO 2 effect on water-use efficiency of temperate forests. *Glob. Chang. Biol.* 1–12. https://doi.org/10.1111/gcb.15491 (2021).
25. Huang, M. et al. Seasonal responses of terrestrial ecosystem water-use efficiency to climate change. *Glob. Chang. Biol.* **22**, 2165–2177 (2016).
26. Guerrieri, R., Lepine, L., Asbjornsen, H., Xiao, J. & Ollinger, S. V. Evapotranspiration and water use efficiency in relation to climate and canopy nitrogen in U.S. forests. *J. Geophys. Res. Biogeosciences* **121**, 2610–2629 (2016).
27. Ponce Campos, G. E. et al. Ecosystem resilience despite large-scale altered hydroclimatic conditions. *Nature* **494**, 349–352 (2013).
28. Dekker, S. C., Groenendijk, M., Booth, B. B. B., Huntingford, C. & Cox, P. M. Spatial and temporal variations in plant water-use efficiency inferred from tree-ring, eddy covariance and atmospheric observations. *Earth Syst. Dyn.* **7**, 525–533 (2016).
29. Tang, J., Luyssaert, S., Richardson, A. D., Kutsch, W. & Janssens, I. A. Steeper declines in forest photosynthesis than respiration explain age-driven decreases in forest growth. *Proc. Natl. Acad. Sci. USA.* **111**, 8856–8860 (2014).
30. Knauer, J. et al. The response of ecosystem water-use efficiency to rising atmospheric CO2 concentrations: sensitivity and large-scale biogeochemical implications. *New Phytol* **213**, 1654–1666 (2017).
31. Fu, L., Xu, Y., Xu, Z., Wu, B. & Zhao, D. Tree water-use efficiency and growth dynamics in response to climatic and environmental changes in a temperate forest in Beijing, China. *Environ. Int.* **134**, 1–10 (2020).
32. Wolf, S. et al. Warm spring reduced carbon cycle impact of the 2012 US summer drought. *Proc. Natl. Acad. Sci. USA.* **113**, 5880–5885 (2016).
33. Buermann, W. et al. Widespread seasonal compensation effects of spring warming on northern plant productivity. *Nature* **562**, 110–114 (2018).
34. Cheng, L. et al. Recent increases in terrestrial carbon uptake at little cost to the water cycle. *Nat. Commun.* **8**, 1–10 (2017).

35. Wang, M., Chen, Y., Wu, X. & Bai, Y. Forest-Type-Dependent Water Use Efficiency Trends Across the Northern Hemisphere. *Geophys. Res. Lett.* **45**, 8283–8293 (2018).
36. Law, B. E. et al. Land use strategies to mitigate climate change in carbon dense temperate forests. *Proc. Natl. Acad. Sci. USA.* **115**, 3663–3668 (2018).
37. Griscom, B. W. et al. National mitigation potential from natural climate solutions in the tropics. *Philos. Trans. R. Soc. B Biol. Sci.* **375**, 1–11 (2020).
38. Schelhaas, M. J. et al. Alternative forest management strategies to account for climate change-induced productivity and species suitability changes in Europe. *Reg. Environ. Chang.* **15**, 1581–1594 (2015).
39. Silva, C. H. L. et al. Persistent collapse of biomass in Amazonian forest edges following deforestation leads to unaccounted carbon losses. *Sci. Adv.* **6**, 1–10 (2020).
40. Teuling, A. J. et al. Climate change, reforestation/afforestation, and urbanization impacts on evapotranspiration and streamflow in Europe. *Hydrol. Earth Syst. Sci.* **23**, 3631–3652 (2019).
41. Duveneck, M. J. & Thompson, J. R. Climate change imposes phenological trade-offs on forest net primary productivity. *J. Geophys. Res. Biogeosciences* **122**, 2298–2313 (2017).
42. Ballantyne, A. et al. Accelerating net terrestrial carbon uptake during the warming hiatus due to reduced respiration. *Nat. Clim. Chang.* **7**, 148–152 (2017).
43. Song, Q. H. et al. Water use efficiency in a primary subtropical evergreen forest in Southwest China. *Sci. Rep.* **7**, 3–12 (2017).
44. Mathias, J. M. & Thomas, R. B. Global tree intrinsic water use efficiency is enhanced by increased atmospheric CO2 and modulated by climate and plant functional types. *Proc. Natl. Acad. Sci. U. S. A.* **118**, 1–9 (2021).
45. Guerrieri, R. et al. Climate and atmospheric deposition effects on forest water-use efficiency and nitrogen availability across Britain. *Sci. Rep.* **10**, 1–16 (2020).
46. Guerrieri, R. et al. Disentangling the role of photosynthesis and stomatal conductance on rising forest water-use efficiency. *Proc. Natl. Acad. Sci. USA.* **116**, 16909–16914 (2019).
47. Adams, M. A., Buckley, T. N. & Turnbull, T. L. Diminishing CO2-driven gains in water-use efficiency of global forests. *Nat. Clim. Chang.* **10**, 466–471 (2020).
48. Soh, W. K. et al. Rising CO2 drives divergence in water use efficiency of evergreen and deciduous plants. *Sci. Adv.* **5**, 1–11 (2019).
49. Keenan, T. F. et al. Increase in forest water-use efficiency as atmospheric carbon dioxide concentrations rise. *Nature* **499**, 324–327 (2013).
50. Fu, Z. et al. Sensitivity of gross primary productivity to climatic drivers during the summer drought of 2018 in Europe: Sensitivity of GPP to climate drivers. *Philos. Trans. R. Soc. B Biol. Sci.* **375**, 1–11 (2020).
51. Frank, D. C. et al. Water-use efficiency and transpiration across European forests during the Anthropocene. *Nat. Clim. Chang.* **5**, 579–583 (2015).
52. Büttner, G. et al. Copernicus Land Monitoring Service-CORINE Land Cover-User Manual. *Copernicus Publications* **1**, 1–129 (2021).
53. Reyer, C. et al. Projections of regional changes in forest net primary productivity for different tree species in Europe driven by climate change and carbon dioxide. *Ann. For. Sci.* **71**, 211–225 (2014).
54. Senf, C., Buras, A., Zang, C. S., Rammig, A. & Seidl, R. Excess forest mortality is consistently linked to drought across Europe. *Nat. Commun.* **11**, 1–8 (2020).
55. Manning, C. et al. Increased probability of compound long-duration dry and hot events in Europe during summer (1950–2013). *Environ. Res. Lett.* **14**, 094006 (2019).
56. Van Der Schrier, G., Van Den Besselaar, E. J. M., Klein Tank, A. M. G. & Verver, G. Monitoring European average temperature based on the E-OBS gridded data set. *J. Geophys. Res. Atmos.* **118**, 5120–5135 (2013).
57. Sulman, B. N. et al. High atmospheric demand for water can limit forest carbon uptake and transpiration as severely as dry soil. *Geophys. Res. Lett.* **43**, 9686–9695 (2016).
58. Yuan, W. et al. Increased atmospheric vapor pressure deficit reduces global vegetation growth. *Sci. Adv.* **5**, 1–13 (2019).
59. Bastos, A. et al. Direct and seasonal legacy effects of the 2018 heat wave and drought on European ecosystem productivity. *Sci. Adv.* **6**, 1–14 (2020).
60. Lindroth, A. et al. Effects of low thinning on carbon dioxide fluxes in a mixed hemiboreal forest. *Agric. For. Meteorol.* **262**, 59–70 (2018).
61. Puhlick, J. J., Weiskittel, A. R., Kenefic, L. S., Woodall, C. W. & Fernandez, I. J. Strategies for enhancing long-term carbon sequestration in mixed-species, naturally regenerated Northern temperate forests. *Carbon Manag* **11**, 381–397 (2020).
62. Duffy, K. A. et al. How close are we to the temperature tipping point of the terrestrial biosphere? *Sci. Adv.* **7**, 1–9 (2021).
63. Sperlich, D. et al. Gains or losses in forest productivity under climate change? The uncertainty of CO2 fertilization and climate effects. *Climate* **8**, 1–22 (2020).
64. Ionita, M., Nagavciuc, V., Kumar, R. & Rakovec, O. On the curious case of the recent decade, mid-spring precipitation deficit in central Europe. *npj Clim. Atmos. Sci.* **3**, 1–10 (2020).
65. Trenberth, K. E. et al. Global warming and changes in drought. *Nat. Clim. Chang.* **4**, 17–22 (2014).
66. Martínez-García, E. et al. Aboveground autotrophic respiration in a Spanish black pine forest: Comparison of scaling methods to improve component partitioning. *Sci. Total Environ.* **580**, 1505–1517 (2017).
67. Wang, X. et al. Soil respiration under climate warming: Differential response of heterotrophic and autotrophic respiration. *Glob. Chang. Biol.* **20**, 3229–3237 (2014).
68. Waring, R. H., Landsberg, J. J. & Williams, M. Net primary production of forests: a constant fraction of gross primary production? *Tree Physiol.* **18**, 129–134 (1998).
69. Collalti, A. & Prentice, I. C. Is NPP proportional to GPP? Waring's hypothesis 20 years on. *Tree Physiol.* **39**, 1473–1483 (2019).
70. Parente, L., Witjes, M., Hengl, T., Landa, M., Brodsky, L. Continental Europe land cover mapping at 30m resolution based CORINE and LUCAS on samples. https://doi.org/10.5281/zenodo.4725429 (2021).
71. Fisher, R. A. & Koven, C. D. Perspectives on the Future of Land Surface Models and the Challenges of Representing Complex Terrestrial Systems. *J. Adv. Model. Earth Syst.* **12**, 1–24 (2020).
72. Zhang, Y. et al. A global moderate resolution dataset of gross primary production of vegetation for 2000–2016. *Sci. data* **4**, 170165 (2017).
73. Zhang, Y. et al. Coupled estimation of 500 m and 8-day resolution global evapotranspiration and gross primary production in 2002–2017. *Remote Sens. Environ.* **222**, 165–182 (2019).
74. Yang, S. et al. The potential of remote sensing-based models on global water-use efficiency estimation: An evaluation and intercomparison of an ecosystem model (BESS) and algorithm (MODIS) using site level and upscaled eddy covariance data. *Agric. For. Meteorol.* **287**, 107959 (2020).
75. Funk, J. M. et al. Securing the climate benefits of stable forests. *Clim. Policy* **19**, 845–860 (2019).
76. Senf, C. & Seidl, R. Mapping the forest disturbance regimes of Europe. *Nat. Sustain.* 63–70 https://doi.org/10.1038/s41893-020-00609-y (2020).
77. Kennedy, R. E., Yang, Z. & Cohen, W. B. Detecting trends in forest disturbance and recovery using yearly Landsat time series: 1. LandTrendr - Temporal segmentation algorithms. *Remote Sens. Environ.* **114**, 2897–2910 (2010).
78. Hofmeister, J. et al. Microclimate edge effect in small fragments of temperate forests in the context of climate change. *For. Ecol. Manage.* **448**, 48–56 (2019).
79. Monteith, J. L. Solar Radiation and Productivity in Tropical Ecosystems. *J. Appl. Ecol.* **9**, 747 (1972).
80. Mu, Q., Zhao, M. & Running, S. W. Improvements to a MODIS global terrestrial evapotranspiration algorithm. *Remote Sens. Environ.* **115**, 1781–1800 (2011).
81. Running, S. W. et al. A continuous satellite-derived measure of global terrestrial primary production. *Bioscience* **54**, 547–560 (2004).
82. Zhao, M., Heinsch, F. A., Nemani, R. R. & Running, S. W. Improvements of the MODIS terrestrial gross and net primary production global data set. *Remote Sens. Environ.* **95**, 164–176 (2005).
83. Running, S. W., Mu, Q., Zhao, M. & Moreno, A. User's Guide MODIS Global Terrestrial Evapotranspiration (ET) Product (MOD16A2/A3 and Year-end Gap-filled MOD16A2GF/A3GF) NASA Earth Observing System MODIS Land Algorithm (For Collection 6). 36 (2019).
84. Running, S. W. & Zhao, M. User's Guide Daily GPP and Annual NPP (MOD17A2H/A3H) and Year-end Gap- Filled (MOD17A2HGF/A3HGF) Products NASA Earth Observing System MODIS Land Algorithm. 1–37 (2019).
85. Pastorello, G. et al. The FLUXNET2015 dataset and the ONEFlux processing pipeline for eddy covariance data. *Sci. Data* **7**, 225 (2020).
86. Anderson, L. O. et al. Vulnerability of Amazonian forests to repeated droughts. *Philos. Trans. R. Soc. B Biol. Sci.* **373**, 20170411 (2018).
87. Montibeller, B., Jaagus, J., Mander, Ü. & Uuemaa, E. Evapotranspiration intensification over unchanged temperate vegetation in the Baltic countries is being driven by climate shifts. *Front. For. Glob. Chang.* **4**, 1–13 (2021).
88. Marshall, M., Okuto, E., Kang, Y., Opiyo, E. & Ahmed, M. Global assessment of Vegetation Index and Phenology Lab (VIP) and Global Inventory Modeling and Mapping Studies (GIMMS) version 3 products. *Biogeosciences* **13**, 625–639 (2016).
89. Berner, L. T. et al. Summer warming explains widespread but not uniform greening in the Arctic tundra biome. *Nat. Commun.* **11**, 4621 (2020).
90. Mann, H. B. Non-parametric test against trend. *Econometrica* **13**, 245–259 (1945).
91. Kendall, M. G. Rank Correlation Methods. *Biometrika* **44**, 298 (1957).
92. Basso, B., Martinez-Feria, R. A., Rill, L. & Ritchie, J. T. Contrasting long-term temperature trends reveal minor changes in projected potential evapotranspiration in the US Midwest. *Nat. Commun.* **12**, 1476 (2021).

Acknowledgements

B.M. and E.U. were funded by the Mobilitas+ programme grant no. MOBERC34 from the Estonian Research Council, and Ü.M. was funded by grant no. PRG352 from the Estonian Research Council and European Regional Development Fund (EcolChange Centre of Excellence) and by grant no. MOBERC44. We thank the anonymous reviewers who helped improving the manuscript.

Author contributions

B.M. and M.M. conceived the study. B.M., E.U. and M.M. wrote the manuscript. B.M. performed the data analysis, with support from E.U., M.M. and Ü.M. All authors approved the manuscript for submission.

Competing interests

The authors declare no competing interests.

Additional information

Supplementary information The online version contains supplementary material available at https://doi.org/10.1038/s43247-022-00535-1.

Correspondence and requests for materials should be addressed to Bruno Montibeller.

Peer review information *Communications Earth & Environment* thanks the anonymous reviewers for their contribution to the peer review of this work. Primary Handling Editors: Gerald Forkuor and Clare Davis. Peer reviewer reports are available.

Reprints and permission information is available at http://www.nature.com/reprints

Publisher's note Springer Nature remains neutral with regard to jurisdictional claims in published maps and institutional affiliations.